A Study on the Torque Performance to Capacitance of a Capacitor-run type Single Phase Induction Motor

Cherl-Jin Kim† , Chul-Yong Choi* and Soo-Hyun Baek**

Abstract - Various kinds of practical machines using the single phase induction motor (SPIM) are utilized to control both speed and torque. In particular, the capacitor-run type SPIM has the characteristic that allows the motor torque to be altered by auxiliary capacitance variation. In this study, we manifest an equivalent model having a more simplified configuration, and clarify the relationship between torque and capacitance. Also, we design an experimental controller that is able to perform speed control with ease by the phase angle control of the AC input voltage. Validity of this study is confirmed through the simulation and experimental results obtained.

Keywords: single phase , induction motor , torque analysis, SPIM, capacitor-run, current phase

1. Introduction

The SPIM is used in common power devices such as most types of general electric in-home appliances. But this kind of motor cannot achieve the rotational magnetic field by itself since it is unable to start up, making it different from the three phase induction type machine.

However, by connecting the capacitor in series with the auxiliary winding, which is parallel connected to the main winding, the current phase of auxiliary winding becomes the leading phase permitting the start of the SPIM. After starting, it generates a pulsated magnetic field as the time passes, and the torque is produced continuously by this magnetic field.

We must consider the generated torque characteristics of driving when optional capacitance is selected for this SPIM, because the starting torque is relatively low in cases of low capacitance. If excessively large capacitance is applied to the SPIM during starting and normal running conditions, efficiency is remarkably decreased to no load or light load. Furthermore, there is the concern of saturation of auxiliary winding and magnetic vibration by unstable driving. Thus the appropriate selection of capacitance should be paid close attention to.

In this study, the torque performance to capacitance variation is analyzed based on the phase analysis of the proposed equivalent model. In this model, both voltage and current of capacitor run type SPIM are divided by the positive or negative phase substance. As well, the generated torque is altered by capacitance and this relation is able to be predicted by MATLAB simulation. In this paper, the above mentioned phenomena are analyzed by computer simulation and confirmed by experiments of a self-designed speed controller using a TRIAC device.

The validity of the proposed model and torque analysis depending on capacitance are verified by comparison and consideration through simulation and experiments.

† Corresponding Author: Dept. of Electrical Eng. Halla University, Wonju, Korea (jkim@hit.halla.ac.kr)
* R&D Center Nara Tech Co., LTD., Kyunggido, Korea (nara@dongguk.edu)
** Dept. of Electrical Eng. Dongguk University, Seoul, Korea
Received April 12, 2004 ; Accepted November 17, 2004

2. Capacitor-run type SPIM

2.1 Motor Characteristics

The capacitor-run type SPIM is able to start and rotate continuously, according to the capacitor that is connected in series with the auxiliary winding, until the phase difference of 90° appears between the main and auxiliary winding. Fig. 1 represents the equivalent circuit of the capacitor-run type SPIM applied to this study. Here, Z_f indicates forward impedance and Z_b indicates backward impedance. The voltage is induced at the main and auxiliary winding by the magnetic field as shown in Equation (1).

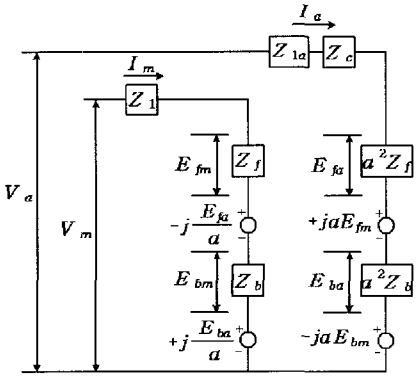

Fig. 1 Equivalent circuit of SPIM

$$\begin{aligned} E_{fm} &= I_m Z_f \\ E_{bm} &= I_m Z_b \\ E_{fa} &= I_a a^2 Z_f \\ E_{ba} &= I_a a^2 Z_b \end{aligned} \tag{1}$$

Here, a is the winding ratio that is equal to the induced voltage ratio of the auxiliary winding to the main winding. The reflected voltage to the main winding is induced by the magnetic field of the auxiliary winding, whose voltage is $1/a$ times that produced in the auxiliary winding. However, because of the spatial relative position of the two windings, the induced voltage of the main winding by the positive direction field of auxiliary winding is 90° delayed. Therefore, the induced voltage of the main winding is delayed by comparison with the positive direction voltage of the auxiliary winding. Furthermore, the induced voltage to the main winding by the negative direction field of the auxiliary winding is 90° ahead by comparison with the induced voltage to the auxiliary winding by the same magnetic field.

The mutual relations of the above mentioned voltage are shown in Equation (2). Here, the currents are divided by main winding and auxiliary winding components and this relation is simplified in Equation (3).

$$\begin{aligned} V_m &= I_m Z_1 + I_m Z_f - jaI_a Z_f + I_m Z_b + jaI_a Z_f \\ V_a &= I_a Z_{1a} + I_a Z_c + a^2 I_a Z_f + jaI_m Z_f + a^2 I_a Z_b + jaI_m Z_b \end{aligned} \tag{2}$$

$$\begin{aligned} I_m &= \frac{V_m Z_{Ta} + jV_a a(Z_f - Z_b)}{Z_T Z_{Ta} - a^2 (Z_f - Z_b)^2} \\ I_a &= \frac{V_a Z_T - jV_m a(Z_f - Z_b)}{Z_T Z_{Ta} - a^2 (Z_f - Z_b)^2} \end{aligned} \tag{3}$$

2.2 Induction of Occurrence Torque

Induced voltage to the main winding by the magnetic field of positive and negative directions is indicated by Equation (4).

$$\begin{aligned} E_f &= (I_m - jaI_a) Z_f \\ E_b &= (I_m + jaI_a) Z_b \end{aligned} \tag{4}$$

Fig. 2 presents the phase relation of currents in the capacitor-run type SPIM.

The torque produced by both magnetic fields is calculated from multiplying the squared current by the resistance caused by each magnetic field. Here, currents by the positive and negative directed magnetic fields are shown respectively in Fig. 2, and the phase ϕ signifies the phase difference of the current between the main and auxiliary winding.

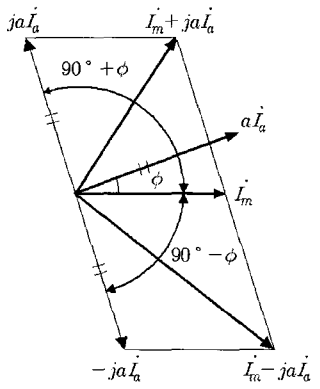

Fig. 2 Current phase of SPIM

Since the driving torque in the capacitor-run type SPIM is produced by the difference between the positive and negative directed torque, the total produced torque is represented by Equation (6).

$$\begin{aligned} T_f &= [I_m^2 + (aI_a)^2 + 2aI_m I_a \sin\phi] R_f \\ T_b &= [I_m^2 + (aI_a)^2 - 2aI_m I_a \sin\phi] R_b \end{aligned} \tag{5}$$

$$\begin{aligned} T &= T_f - T_b \\ &= \frac{\{I_m^2 + (aI_a)^2\}(R_f - R_b) + (2aI_m I_a \sin\phi)(R_f + R_b)}{\omega_{syn}} \end{aligned} \tag{6}$$

3. Characteristics Analysis

3.1 Characteristics Analysis by the Parameter

In this study, torque performance depending on capacitance change is analyzed using (6).

The applied motor for analysis is the 4 pole, 40[W] type, and the parameters based on the motor's basic data are simulated by the analyzing program. The detailed parameters of the capacitor-run type SPIM, which are acquired from the physical design data and material specification, are presented in Table 1.

Table 1 Parameters of the Motor

Parameter	Numerical value
Main-Phase Resistance (ohm)	63.5729
Aux.-Phase Resistance (ohm)	76.202
Main Leakage Reactance (ohm)	49.8734
Aux. Leakage Reactance (ohm)	71.0875
Rotor Resistance (ohm)	199.895
Rotor Leakage Reactance	82.2302
Magnetizing Reactance	849.654
Turn Ratio of Aux. to Main-Coil	1.09155
Rated Slip	0.2775

The phase angle difference between the main and auxiliary winding is occurred from the capacitance of auxiliary winding. Fig. 3 represents the torque simulation results according to capacitance variation. It is found that the maximum torque is produced close to 90°.

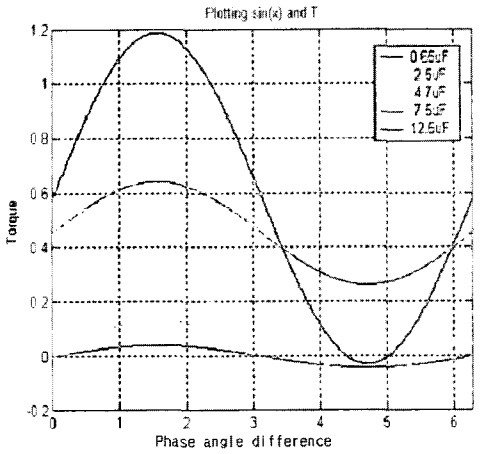

Fig. 3 Phase angle to Torque curve for capacitance

Fig. 4 shows the simulation results of output torque characteristics depending on each capacitance. Here, it is known that the maximum torque is increased gradually until optional capacitance (in this case, 7.5 μF) as capacitance increases. On the other hand, produced torque is decreased above this optional capacitance in this capacitor-run type SPIM.

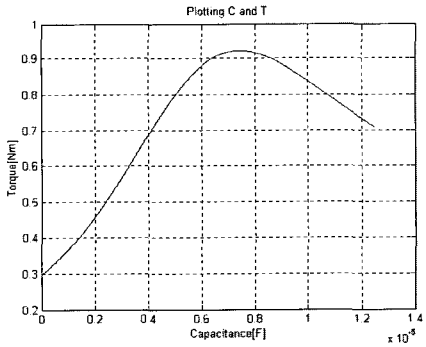

Fig. 4 Capacitance-Torque curve according to value of capacitor

3.2 Characteristics Analysis by 2D FEM

The FEM (Finite Element Method) is a very useful tool when used together with the multi-purpose numerical analysis method, which uses various application fields to interpret electromagnetic phenomena.

In this study, we composed a 2D shape for interpretation to apply the basic parameters of the capacitor-run type SPIM (40[W], 4 pole), and we used commercialized packages such as RM-Xprt and Em-pulse (2D).

The parameters of the target motor model are expressed as shown in the following Table 1. The basic specifications and structure are expressed as Table 2 and Fig. 5, respectively.

Table 2 Specifications of capacitor-run type SPIM

Rated output power [W]	40
Rated voltage [V]	220
Pole pairs	4
Frequency [Hz]	60
Rated speed [rpm]	1550

Fig. 5 indicates the structure of the applied SPIM, which is composed of a stator and a rotor with fitted slots. The material of the stator is si-steel and rotor conductor is aluminum. Winding distribution is expressed as in Fig. 6.

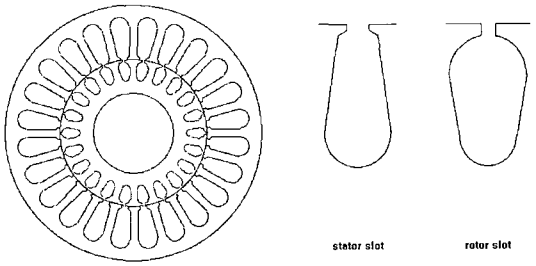

Fig. 5 SPIM structure

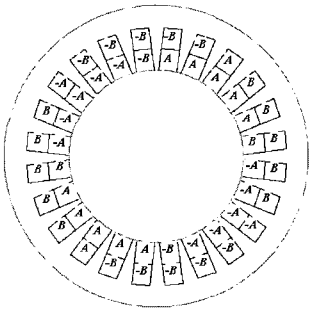

Fig. 6 Winding distribution of SPIM

In this study, the magnetic path of the target motor is divided into 1,075 elements, and the analysis result of flux density distribution using a software package is presented in Fig. 7.

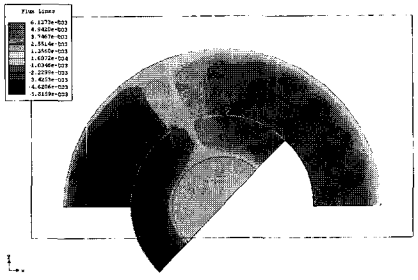

Fig. 7 Magnetic flux density of SPIM

The flux distribution results according to the capacitance variation are expressed in Fig. 8.

From the simulation results, we found that the capacitance of the maximum torque generation region (7.5 μF) and the most stable operation (2.5 μF) region are different values. The reason for this is that unnecessary flux is present nearby the shaft area with excessive capacitance.

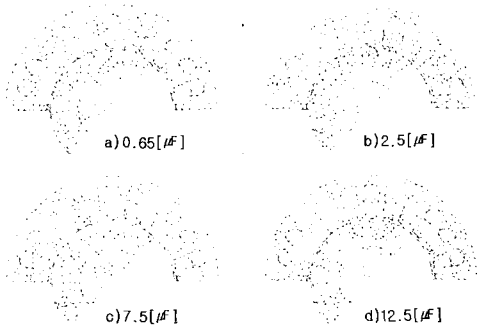

Fig. 8 Flux density distribution of capacitor-run type SPIM

3.3 Characteristics Analysis by phase diagram

The phase diagram is used with capacitance variation for easy analysis, and we obtained the respective characteristics from the simulation results of phase difference between each winding current in the capacitor-run type SPIM as indicated in Fig. 9.

From these phase diagram analyses, we obtained results indicating that the phase angle difference is nearly 90 degrees between the main winding and auxiliary winding at 2.5 μF capacitance, that is, 2.5 μF is the most adequate capacitance in this study.

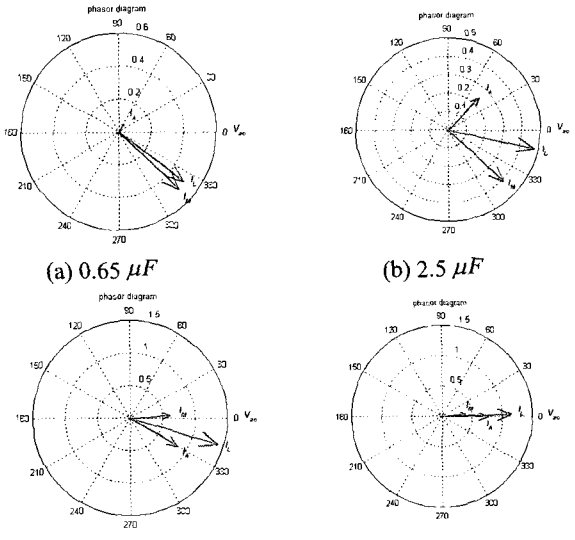

(a) 0.65 μF (b) 2.5 μF

(c) 7.5 μF (d) 12.5 μF

Fig. 9 Phase diagram of main and auxiliary winding currents with various capacitances

4. Experiment Results and Consideration

Fig. 10 represents the circuit composition of the experimental speed controller for this study. Above all, the CPU is interrupted by the detected zero-voltage signal in this circuit. Then the proper phase angle, which is applicable to the desired speed, is calculated by the control algorithm. After initiating operation, the CPU produces a trigger signal to the main switching device (TRIAC) and electric energy is supplied to the motor.

The capacitance-torque and speed-torque performance simulation results are compared with the experimental results as capacitance is changed with 0.65-12.5 μF .

The starting torque ($s = 1$) is simulated in Fig. 4 and running torque is simulated in Fig. 11. It is known that the torque curve shape is mutually similar to capacitance variation from these simulation results. In this case, the proper capacitance is 7.5 μF .

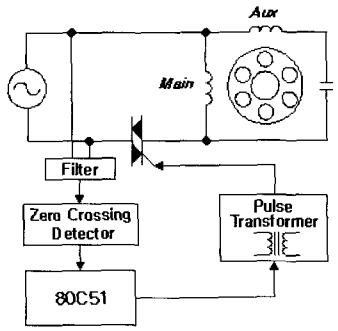

Fig. 10 Speed controller diagram with phase control method

If capacitance is higher than 7.5 μF , vibration, heat dissipation and noise are generated in the test motor. As this actual fact has been previously predicted by simulation, it is very important to determine the exact capacitance in the capacitor-run type SPIM, therefore great attention must be paid to capacitor selection.

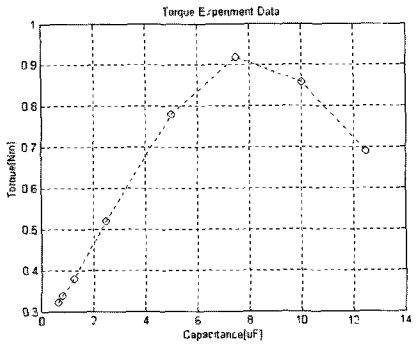

Fig. 11 Torque characteristic experiment

Fig. 12 presents the experimental results of current measurement between the main and auxiliary windings

according to capacitance variation. According to test results, it is established that phase differences are gradually changed as capacitance increases.

In Fig. 12, torque and current are rapidly increased just as capacitance is increased like in the prediction of Fig. 3. And noise and vibration phenomena are represented above 7.5 μF in the test.

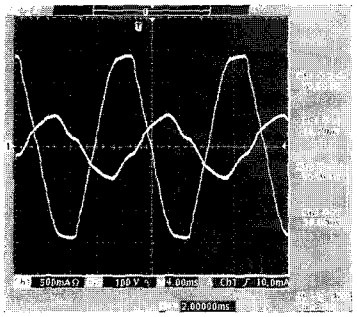

(a) 2.5 μF

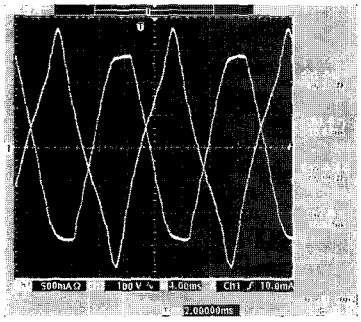

(b) 7.5 μF

Fig. 12 Current waveforms of main and auxiliary winding

A cause of noise and vibration is able to be estimated at harmonics generated by TRIAC switching for phase control. The test result of harmonics included in input current is represented by FFT analysis in Fig. 13, here applied capacitance is 2.5 μF and 7.5 μF respectively.

As in figure 13, the harmonics in 7.5 μF is greater than the 2.5 μF case. In particular, the third harmonics is increased about 75[%] comparing the fundamental component in 7.5 μF.

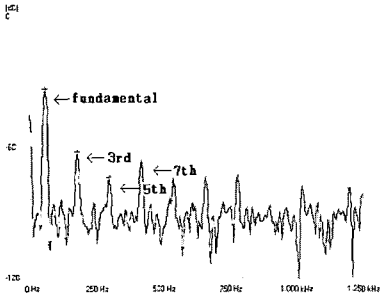

(a) 2.5 μF

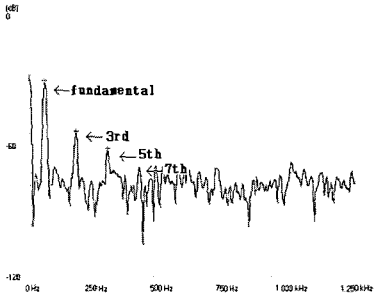

(b) 7.5 μF

Fig. 13 Experimental results of harmonic analysis

Fig. 14 and Fig. 15 represent speed-torque characteristics to capacitance variation 0.65-12.5 μF . It is confirmed that starting torque increases in proportion to capacitance, and the maximum torque moves toward low speed range. In the case of this study, the maximum torque is occurred at 7.5 μF , and torque decreases gradually above 7.5 μF as per the prediction of the simulation. But, the noise and vibration are generated slightly in 7.5 μF . Therefore it is recommendable to have capacitance slightly lower than 7.5 μF for stable operation and for preventing decline in efficiency.

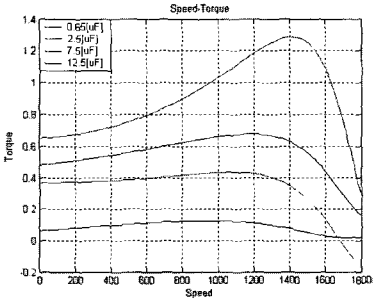

Fig. 14 Simulation of speed-torque curve

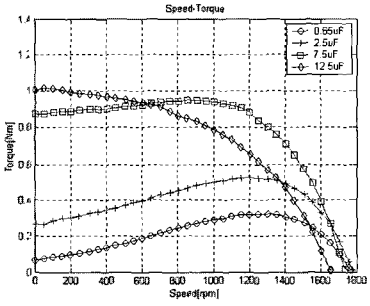

Fig. 15 Experiment of speed–torque curve

Fig. 16 represents efficiency characteristics in accordance with speed change and capacitance variation by MATLAB simulation.

From the comparison results regarding speed-efficiency to each capacitance, it is determined that the efficiency in 2.5 μF is higher than that in 7.5 μF .

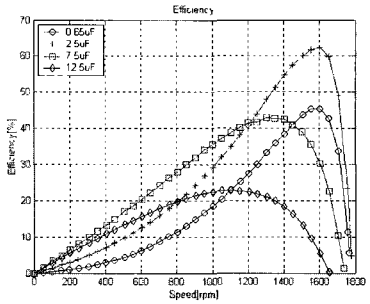

Fig. 16 Efficiency for capacitance

5. Conclusions

The output of the capacitor-run type SPIM is decided by various parameters such as capacitance and phase angle.

In this paper, the voltage and current of the capacitor-run type SPIM are divided by positive and negative phase, based on a two motor theory.

We simulated the torque characteristics with capacitance variation from the equivalent circuit of a single phase induction motor.

In this analysis, the torque equation with capacitance variation is induced, and theoretical simulation is carried out by the MATLAB program.

Flux density distribution was studied by the commercial FEM analyzing package with various capacitances. The phase diagram of the main and auxiliary winding currents was also expressed.

From this observation, 2.5 μF capacitance was proper to the relative ideal drive of this target motor with a 90 degree phase difference between the main and auxiliary windings.

To confirm the validity of the theoretical analyzing result, we experimented using an actual motor (220[v], 4 pole, 40[W]). From the results of torque characteristics to the capacitance variation, the maximum torque occurred close to 7.5 μF , but this capacitance was less efficient compared to the 2.5 μF capacitance due to the flux dispersion of the surrounding shaft and below the 90 degree phase difference.

We found that the proper capacitance maintained nearly a 90 degree phase difference guarantee than the higher efficiency and the excessive capacitance generated unwanted vibration and noise.

In the near future, a very useful adaptation is expected in many industrial fields that will apply the capacitor-run type SPIM, by the development of a more generalized design method based on this study.

Acknowledgements

This work has been supported by KESRI, which is funded by MOCIE(Ministry of commerce, industry and energy).

References

[1] Leander W. Matsch, Electromagnetic & Electromechanical Machines, IEP, pp. 445-471, 1977.

[2] 三宅 博 著, 小形 AC モータの設計と制御, 總合電子出版社, pp. 1-189, 1984

[3] Joon-Hyoung Rye, Kwang-Won Lee, "Speed Control of Capacitor-Run Induction Motor Using Voltage Control of the Auxiliary Winding", KIEE, Vol. 48B, No. 7, pp. 357-362, July. 1999.

[4] Sang-Baeck Yoon, Jung-Pyo Hong, "Construction of Equivalent Circuit Characteristic Analysis of Permanent-Split Condenser Induction Motor", KIEE, Vol. 45, No. 9, Sept. 1996.

[5] Jung-Pyo Hong "Circuit Parameters and Characteristic Analysis of Condenser Run Single Phase Induction Motor by Combine Equivalent Circuit with Numerical Method" KIEE, Vol. 49B, No. 11, Nov. 2000.

[6] H. Huang, E. F. Fuchs, J. C. White, "Optimal Placement of the Run-Capacitor in Single-Phase Induction Motor Designs", IEEE, Vol. 3, No. 3, pp. 647-652, 1988.

[7] E. R. Colins, Jr. "Operating Characteristics of Single-Phase Capacitor Motors Driven from Variable Frequency Supplies", IEEE IAS'91, pp. 52-57, 1991.

[8] Eduard Muljadi, "Adjustable ac Capacitor for a Single-Phase Induction Motor", IEEE, Vol. 29, No. 3, pp. 479-485, 1993.

[9] E. R. Colins, Jr. "Improved methods for determining the equivalent circuit parameters for single-phase induction motor models", IEEE IAS'93, pp. 390-395, 1993.

Cherl-Jin Kim,
He received his B.S., M.S. and Ph.D. degrees in Electrical Engineering from Hanyang University, Seoul, Korea during the period of 1980 to 1991. From 1991 to 1995, he was with the Korea Electronics Technology Institute where he became Head Researcher of the Control Systems Laboratory. Since 1995, he has been with Halla University as a Professor in the Electrical Engineering Department. His research activities are in the area of power electronics, which includes electrical machine control systems and static converter design fields.
Tel: 82-2-2260-3347 Fax: 82-02-2263-4625

Chul-Yong Choi

He received his B.S. degree in Electrical Engineering from Halla University, Wonju, Kangwon, Korea during the period of 1998 to 2002. He received his M.S. degree in Electrical Engineering from Dongguk University, Seoul, Korea during the period of 2002 to 2004. Since 2004, he has been with Qualiflow Naratech Co. LTD. as a Researcher in the R&D Center. His research activities are in the area of motor control, which includes power electronics and electrical machine control systems.

Soo-Hyun Baek

He received his B.S., M.S and Ph.D. degrees in Electrical Engineering from Hanyang University in 1972, 1974 and 1983, respectively. Since 1977, he has been a Professor in the Department of Electrical Engineering at Dongguk University, Seoul, Korea. He has been a member of both the KIEE and ICEE. His major research interests are in the areas of renewal energy conversionary systems, motor control systems, power electronics, ultrasonic motors, and the design and analysis of electrical machines.